DFT, SERS, and single-molecule SERS of crystal violet

ARTICLE *in* THE JOURNAL OF PHYSICAL CHEMISTRY C · DECEMBER 2008

Impact Factor: 4.77 · DOI: 10.1021/jp807807j

DFT, SERS, and Single-Molecule SERS of Crystal Violet

Maria Vega Cañamares,* Cat Chenal, Ronald L. Birke, and John R. Lombardi

Department of Chemistry and Center for Analysis of Structures and Interfaces (CASI), The City College of New York, New York, New York 10031

Received: September 02, 2008; Revised Manuscript Received: October 30, 2008

Applying the method of density functional theory calculations, we examine the Raman and surface-enhanced Raman spectra (SERS) of crystal violet. The resulting optimized structure is of point symmetry D_3, and the calculated Raman spectrum provides an excellent match with the observed normal Raman spectrum. This provides a reliable assignment of the symmetry and normal modes of the observed spectrum, which consists of bands assigned to modes of either a_1 or e symmetry. The e modes are not split, showing that D_3 symmetry remains, even on the surface. The SERS spectra, both normal and single-molecule, are dominated by the nontotally symmetric e vibrations, which are preferentially enhanced in accord with the Herzberg−Teller-surface selection rules. The mechanism involves intensity borrowing through vibronic coupling between a charge-transfer state and the lowest-lying $\pi \rightarrow \pi^*$ transition. A quantitative measure of the degree of charge transfer is obtained by analyzing the potential dependence of SERS intensities. This indicates a considerable contribution of charge-transfer intensity to the overall SERS enhancement.

I. Introduction

Surface-enhanced Raman spectroscopy (SERS) is characterized by a rather large enhancement of the normally weak Raman signal. The origin of this enhancement was shown to rely on a resonance of the laser with a surface plasmon (SPR) in the underlying metal nanostructure. In addition, it was observed that the intrusion of certain charge-transfer (CT) resonances was also needed to provide a complete description of experimental observations.[1] Since the effect was first observed in the late 1970s,[2−4] it had inspired numerous articles spanning the ensuing 20 years. By the late 1990s, SERS was considered a rather mature field. However, the field was rejuvenated by a series of remarkable papers concerning SERS spectra obtained in single-molecule systems[5−8] (SM-SERS). These were observed with one or just a few molecules adsorbed on one, or between two, Ag nanoparticles.[9,10] Such observations could be explained by resorting to Raman enhancement factors as large as 10^{14}. Thus, SM-SERS is expected to become a tool of choice for highly sensitive detection of trace quantities of materials.

In order to detect the Raman spectrum from single molecules, it was originally necessary to take advantage of the additional boost in intensity provided by a molecular resonance, and therefore various dye molecules such as rhodamine 6G (R6G) and crystal violet (CV) were employed. Since then, however, detection of single-molecule spectra has been achieved with lower enhancement factors and molecules which do not necessarily absorb in the region of excitation.[11] In any case, it would be worthwhile to re-examine the SERS and SM-SERS spectra of these dye compounds in order to determine the extent to which the previous views of the enhancement mechanism apply to these new systems. An important issue in this regard is the degree to which each of the various components (i.e., SPR, CT, or molecular resonance) contributes to the overall enhancement.[12] One reliable diagnostic for the contribution of charge transfer is the relative enhancement of nontotally symmetric modes, which obtain their SERS intensity through a Herzberg−Teller vibronic coupling mechanism. It has been shown that in regions of the SERS excitation profile for which only surface plasmon resonances contribute, totally symmetric modes should dominate the spectrum, with only weak, if any, contributions from nontotally symmetric modes. However, in spectral regions where a charge-transfer resonance is involved, nontotally symmetric modes not only are more enhanced but can even dominate the spectrum under certain circumstances. This is the extension to SERS of the well-known fact that Raman spectra differ considerably in relative intensities of lines with differing symmetry depending on whether the laser is in resonance with a molecular transition. Totally symmetric modes tend to be more strongly enhanced near resonances due to Franck−Condon influences,[13] whereas the possibility of nontotally symmetric ("forbidden" intensity) bands[14] may be excited by Herzberg−Teller vibronic coupling.

In the SERS spectrum of rhodamine 6G, there are two lines of interest, namely, the lines at 613 and 775 cm^{-1}. These two lines display the highest and third-highest enhancement in the single-molecule experiments[8] and, since they represent out-of-plane vibrations, are likely candidates for such an examination. The R6G molecule is composed of two parts, one a nearly planar xanthene moiety, to which most of the observed vibrations are assigned. It has been shown that this part of the molecule lies flat on the silver surface,[15] and to the extent that we may approximate it as a planar system, we may consider a plane of symmetry. Then, using the symmetry point group C_s, in-plane vibrations are totally symmetric (a′) and out-of-plane vibrations are nontotally symmetric (a″). Since the charge-transfer transition dipole is perpendicular to the molecular plane (A″), the Herzberg−Teller-surface selection rules[18] predict that a″ (A″ × A′) vibrations will be most strongly enhanced. This is exactly as observed. There are, however, several difficulties with this analysis. First, R6G is not a symmetrical molecule. In fact, in the equilibrium ground state it has no symmetry at all so that the assignment to symmetry species a′ and a″ is an approximation at best. Furthermore, the fact that both lines are nearly

* Corresponding author. Fax: 212-650-6848. Phone: 212-650-6042. E-mail: maria.canamares@metmuseum.org.

10.1021/jp807807j CCC: $40.75
Published on Web 12/03/2008

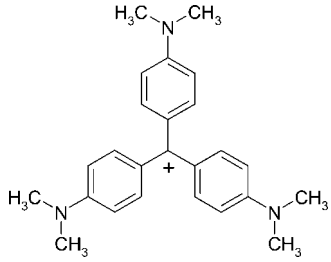

Figure 1. Structure of crystal violet.

coincident with nearby in-plane lines raises questions as to which species is actually responsible for the observed enhancement.

Less ambiguous would be examination of the spectrum of crystal violet (Figure 1), which has much higher symmetry, and therefore should provide a more rigorous test of the unified SERS theory.[12] The first observation of SERS in this system was reported in one of the earliest SERS articles.[4] Crystal violet is a tri-*p*-dimethylaminophenyl carbonium ion, in which the three rings are symmetrically arrayed around a central carbonium atom. X-ray diffraction studies[16] show that the rings do not lie flat in the carbonium plane but are tilted by about 30° in a propeller-like shape. The resulting symmetry point group is D_3. A magnetic circular dichroism study[17] showed that in solution crystal violet is of D_3 symmetry. However, there is considerable controversy as to the correct conformation in the liquid phase, in the presence of certain counterions, or on metal substrates. It is not our intention here to review all the literature on this molecule, but an excellent summary has been provided by Liang et al.[18] Note that the Herzberg−Teller mechanism involves vibronic coupling between vibrational and electronic motions in a molecule. There is a long history of studies of vibronic coupling in crystal violet, mostly concerned with the shoulder[19] in the 600 nm absorption band at 550 nm. This is the same Herzberg−Teller coupling that is implicated in the charge-transfer contributions to SERS.[1,14]

In essence, there are conflicting data, some of which suggest that various perturbing influences can lower the symmetry of the molecule to C_2. For our purposes here, we are especially concerned with two articles in which the polarization dependence of the Raman spectrum is used to determine the ground-state molecular symmetry. In one, Angeloni et al.[20] show that numerous bands are polarized and therefore can be assigned to totally symmetric a_1 vibrations, whereas other depolarized bands are nontotally symmetric e vibrations. These assignments were confirmed by a perdeuterated CV study of Sunder and Bernstein.[21] However, in a nearly identical experiment, Lueck et al.[22] report that all the bands are polarized, and therefore all the normal modes observed are totally symmetric, ruling out D_3 symmetry and suggesting instead C_2. If we are to have an adequate gauge of the charge-transfer contributions to SM-SERS in CV, we must first determine which is the correct symmetry to use. To this end, we utilize the power of density functional theory (DFT) to provide excellent values for normal-mode frequencies and intensities. In recent works,[23−26] we have found that DFT provides a reliable and accurate way to predict and therefore assign Raman spectra of various dye molecules. The close fit to the observed spectra afforded by the DFT method in these and similar cases provides confidence in the reliability of the spectral assignments. By comparison with the FT-Raman spectrum of CV, we are able to improve previous assignments and determine the correct symmetry of the ground state in a SERS experiment. We then use the symmetries of the spectral assignments to analyze the source and magnitude of the contribution of charge-transfer resonance to the SERS enhancement.

II. Experimental Section

Crystal violet, also known as basic violet 3 (CI 42555), was purchased from Sigma. Stock solutions of the dye were prepared by dissolving a few crystals of the dye in 0.5 mL of pure methanol.

The Ag colloid was prepared following the method of Lee and Meisel[27] by reduction of silver nitrate (Aldrich 209139 silver nitrate 99.9%) with sodium citrate (Aldrich W302600 sodium citrate dihydrate). The colloid was concentrated by centrifugation for 2 min at 5000 rpm followed by removal of the supernatant. Only ultrapure water was used for the preparation of the various solutions.

SERS measurement were made simply by adding 0.5 μL of dye solution to a 1 μL drop of colloid deposited on a glass microscope slide, followed by addition of 1 μL of a 0.5 M KNO_3 solution. Raman measurements were taken directly from the drop using a 100× microscope objective and focusing on the microscope slide surface.

The FT-Raman spectrum of CV was obtained directly from the powder. It was carried out using a Bruker Ram II FT-Raman-Vertex 70 FTIR Micro spectrometer. The 1064 nm line of an Nd:YAG laser was used as the excitation line. The resolution was set to 4 cm^{-1} in backscattering mode. A liquid nitrogen cooled Ge detector was used to collect 200 scans for a good Raman spectrum. The laser output was kept at 50 mW.

SERS work on Ag colloids was carried out using a Bruker Senterra Raman microscope using a He−Ne laser at 633 nm, a 1800 rulings/mm holographic grating, a CCD detector, and power at the sample of 10 mW.

Density functional theory calculations were performed with Gaussian 03[28] at the B3LYP level of theory and employing the 6-31G** basis set. The geometry optimization resulted in a nonplanar geometry, and no imaginary frequencies were observed in the calculated spectrum. This basis set was chosen to be consistent with earlier work[24] and because the fit obtained was excellent (see Table 1 and Figure 2). The vibrational normal-mode assignments were based on the best-fit comparison of the calculated Raman spectrum with the observed FT-Raman spectrum, after scaling the calculated wavenumbers. DFT and TD-DFT calculations were also performed to take into consideration the effect of solvent on the energy levels. These calculations were made at the B3LYP/6-31G** level with the conductor polarized continuum model (CPCM), for an aqueous solvent.

III. Results

In Figure 2, we compare the results of the DFT calculation with the observed FT-Raman spectrum taken at 1064 nm. The optimized geometry is D_3 symmetry in agreement with the X-ray crystallographic results.[16] In accord with established procedures[23−26] we have scaled the wavenumber axis by a factor of 0.97 to obtain the best fit. It can be seen that the fit is excellent. Nearly every line is accurately located in both wavenumber and intensity. On this basis, we may have confidence that the assignments listed in the table are indeed correct. The only exceptions are the lines at 1617 and 1582 cm^{-1}, which are predicted to lie about 10−20 cm^{-1} higher in DFT than is actually observed. However, the intensity ratio of these lines is about right, and in relation to the other lines in the spectrum, the assignments are clearly unambiguous. Each of the observed bands may be assigned on the basis of D_3 point group to either an a_1 or e irreducible representation. In columns 4 and 5 of Table 1 we list the benzene mode, which is most closely involved in the vibration, as well as a brief description of other

TABLE 1: DFT and Assignments of FT-Raman, SERS, and SM-SERS of Crystal Violet

DFT (× 0.97)[a]	mode no. DFT (Raman scattering factors)		benzene mode	description of vibrations contributing to the normal mode[b]	FT-Raman[a]	SERS 633 nm[a]	SM-SERS[c]
1627 sh	138 (24)	a_1	8a		1617 w	1620 m	1622
1601 vs	136/137 (623/629)	e	8a		1582 vs	1587 vw	1584
1532 s	134/135 (222/210)	e	8b	$\nu(C_{ring}N)/\delta_s(CH_3)$	1536 w	1535 vw	
1491 w	127/128 (129/130)	e	19a	$\delta_{as}(CH_3)$	1480 vw	1474 vw	
1462 w	119/120 (7/6)	e	19b	$\delta_{as}(CH_3)$	1447 vw	1448 vw	
1380 w	108 (297)	a_1	νø−N)	$\delta(CH)/\delta_s(CH_3)/\delta(CCC)_{ring}$	1390 w	1391 sh	
1360 s	104/105 (398/400)	e	νø−N)	$\nu_{as}(CC_{center}C)/\delta(CCC)_{ring}/\delta(CH)$	1357 s	1377 vs	
1335 w	101/102 (59/60)	e	$\delta(\phi-N)$	$\delta(CCC)_{ring}/\nu_{as}(CC_{center}C)/\delta(CH)$	1338 sh	1336 sh	
1295 vw	99/100 (40/39)	e		$\nu_{as}(CC_{center}C)/\delta(CCC)_{ring}/\delta(CH)$	1299 vw	1298 w	
1233 vw	95/96 (37/37)	e		$\nu(CN)/\rho_r(CH_3)/\delta(CH)$	1228 vw		
1221 sh	94 (20)	a_1		$\nu_s(CC_{center}C)/\delta(CCC)_{breathing}/\delta(CH)$		1220 vw	
1187 w	92/93 (169/170)	e	9a	$\nu_{as}(CC_{center}C)$	1185 m	1175 vs	1176
1165 vw	88 (93)	a_1	9a	$\nu_s(CC_{center}C)/\delta(CCC)_{breathing}/\rho_r(CH_3)$	1170 m		
1137 vw	86/87 (7/7)	e	15	$\delta(CC_{center}C)/\nu CN)$	1133 sh	1123 sh	
984 wv	74/75 (1/1)	e		$\delta(CCC)$	994 vw	996 sh	
952 vw	70 (30)	a_1	17a		973 vw	978 w	
932 vw	64 (55)	a_1	1	$\rho_r(CH_3)/\nu CN)$	940 vw	941 w	
902 vw	62/63 (65/65)	e	17a	$\delta(CC_{center}C)$	915 m	916 m	914
844 vw	59/60 (0/0)	e	17b		821 vw	826 sh	
792 vw	56/57 34/34)	e	10a		803 vw	806 m	804
760 vw	55 (23)	a_1	6a	$\nu_s(CC_{center}C)/\nu(CN)$	767 vw	761 w	
715 w	50/51 (90/91)	e	4	$\nu(CN)$	724 m	726 w	
625 vw	47/48 (2/2)	e	6b		628 vw	623 vw	
603 vw	45 (1)	a_1		$\delta(CCC)/\delta(CNC)/\nu_s(CC_{center}C)$	605 vw	607 vw	
560 vw	43/44 (0/0)	e	6a	$\gamma(CCC)/\delta(CNC)/\delta(CC_{center}C)$	558 vw	561 vw	
522 vw	41/42 (52/50)	e	16b	$\delta(CNC)$	524 w	526 w	
435 vw	35 (8)	a_1	16a	$\delta(CNC)$	437 sh	442 s	
430 vw	33/34 (65/62)	e	16a	$\delta(CNC)/\delta(CC_{center}C)$	418 m	425 m	
337 vw	29/30 (14/14)	e	$\delta(\phi-C-\phi)$	$\gamma(CNC)/\rho_r(CH_3)$	337 w	339 vw	
238 vw	23/24 (7/8)	e	$\delta(\phi-C-\phi)$	$\gamma(CNC)/\rho_r(CH_3)$	227 vw		
202 vw	22 (46)	a_1	breath	$\tau(CH_3)$	204 m	209 vs	

[a] vs, very strong; s, strong; m, medium; w, weak; vw, very weak, sh, shoulder. [b] ν, stretching (s, symmetric; as, asymmetric); δ, bending; γ, out-of-plane deformation (respect to the benzene ring); τ, torsion. [c] These are taken from refs 6 and 8 which essentially agree except the line at 1584 cm^{-1} is reported only in the former.

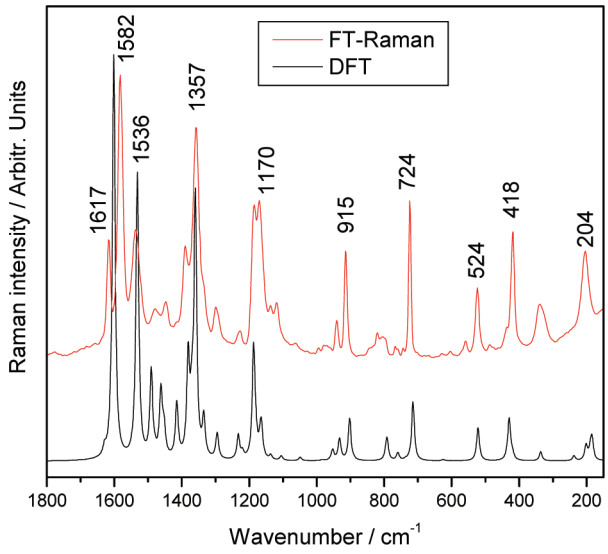

Figure 2. Density functional theory (DFT) calculated spectrum (scaled by 0.97) compared with the FT-Raman spectrum of crystal violet at 1064 nm.

important atomic motions involved in the vibration. Note that each branch of the molecule involves a para-substituted benzene ring and may separately be considered to vibrate accordingly. However, the symmetry requirements imposed by the overall molecular species will produce linear combinations of these to form a set of a_1 and e vibrations. Thus, for every benzene-like mode we expect two distinct spectral bands corresponding to the two types of vibration. We have not listed all of these in the table since they are not all sufficiently intense to be observed in the spectrum. However, this explains why, for example, both the ν_{138} (a_1) and $\nu_{136,7}$ (e) modes at 1617 and 1582 cm^{-1}, respectively, stem from an 8a benzene mode.

With several exceptions our assignments agree with those of Angeloni et al.[20] and Sunder and Bernstein.[21] Most of these exceptions involve disagreements concerning which benzene modes contribute to certain CV modes. These include the band at 994 cm^{-1}, assigned by Angeloni et al. to the symmetric ring breathing (1) mode in benzene. In our case, this mode is assigned to the band at 940 cm^{-1}. Additionally, the normal Raman bands at 973 (17a), 915 (17a), 821 (17b), 767 (6a), 724 (4), and 524 (16b) cm^{-1} were assigned by Angeloni et al.[20] to the 18a, 12, 10b, 17a, 17b, and 6b modes, respectively. Our assignments were made by inspection of the DFT normal-mode display (Gaussview), whereas those of Angeloni et al. were made by analogy with the benzene vibrational wavenumbers and, therefore, are less reliable. Some modes from the DFT output correspond to no identifiable benzene modes. For example, the mode at 605 cm^{-1}, which was assigned by Angeloni et al. to 6a, or the above-mentioned mode at 994 cm^{-1}. Since our main concern here is symmetry, we should point out that our symmetry assignments agree with those of Angeloni et al. in each case. The only disagreement in symmetry is in the band at 803 cm^{-1}. The polarization experiments of Angeloni et al. indicate that it has a_1 symmetry, whereas our DFT calculation gives e symmetry to that vibration. The cause of this discrepancy

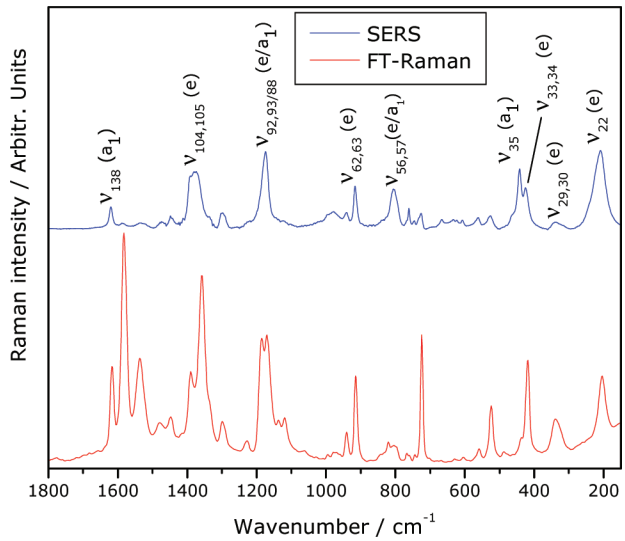

Figure 3. FT-Raman (1064 nm) and SERS (633 nm) on Ag colloid of crystal violet.

is not clear. However, there is a nearby *e* band at 821 cm^{-1}, which may have caused some interference in the depolarization studies. However, we take this symmetry assignment to be unresolved. There is a similar problem with overlap of a_1 and *e* modes at 1185 cm^{-1}.

It should be emphasized that the *e* modes observed here are doubly degenerate and that there is no evidence that this degeneracy is split in solution. This would be necessary in order for the depolarization experiments of Leuck et al.[22] to be correct since in C_2 symmetry there are no degeneracies. If the symmetry lowering perturbation were strong enough to lower the symmetry, the *e* modes would appear as doublets in the solution Raman spectra. In this regard we agree with the conclusions of Angeloni et al.[20] that crystal violet retains D_3 symmetry in solution. There is no evidence of splitting either in the normal Raman or in SERS, nor has such splitting been reported by other researchers.[6,8]

In Figure 3, we show the SERS spectrum of CV on Ag colloid, and the observed wavenumbers are shown in Table 1, where they are also compared to those measured in the single-molecule experiments. By comparison with the FT-Raman spectrum, it can be seen from the figure that although the relative intensities of the lines are drastically altered by proximity to the surface, the observed wavenumbers are not altered much. This suggests that only a weak interaction (physisorption) occurs between the molecule and the Ag nanoparticles. This is consistent with other observations in large dye molecules. Only a few of the low-lying lines associated with the adsorption to the silver surface are shifted perceptibly. One is as the very strong 205 cm^{-1} line shifted to 209 cm^{-1}, which has been attributed to the citrate adduct and may be sensitive to the adsorption of the CV. The other is the line at 1357 cm^{-1}, which shifts up to 1377 cm^{-1}. This has been assigned as the phenyl−N stretch and is also most likely implicated in the adsorption of the molecule to the surface. Presumably, the other lines are less tied to the molecule−metal interaction.

We are now in a position to properly interpret the results of the SM-SERS observations. As can be seen from the last two columns of Table 1, there is agreement between our SERS spectra and the single-molecule results. The most intense of our lines are also seen in the SM-SERS spectra, for which the weaker lines are not reported. The most striking observation is that most of the enhanced lines are assigned as nontotally symmetric *e* modes. Note also that the most intensely enhanced lines, both in the SERS and single-molecule experiments, are of *e* symmetry. In fact the single-molecule line with the largest enhancement factor is the 914 cm^{-1} line (SMEF of 6.9×10^{11}).[8] The next two most enhanced lines (at 804 and 1176 cm^{-1}) are ambiguous in that they are near overlapping of a_1 and *e* vibrations. The line at 1622 cm^{-1} is clearly a_1, whereas that at 1584 cm^{-1} is clearly *e*.

For SERS spectra far from a molecular or charge-transfer resonance, we expect that the totally symmetric (a_1) modes will dominate the spectrum. However, in the region considered here, the nontotally symmetric (*e*) modes are observed to be prominent and constitute a large fraction of the total enhancement. This has been observed in numerous other situations,[12] and in these circumstances it is necessary to examine the vibronic coupling (Herzberg−Teller) contributions to the SERS spectrum. The Herzberg−Teller-surface selection rules[12] for SERS spectra which lie in the region of a molecular resonance may be expressed simply as $\Gamma(Q_k) = \Gamma(\mu_{CT}^{\perp}) \times \Gamma_K$, where $\Gamma(Q_k)$ is the irreducible representation to which an allowed (i.e., strongly enhanced) normal mode (Q_k) belongs. Γ_K is the irreducible representation of the electronic state (K) to which the allowed molecular takes place, and $\Gamma(\mu_{CT}^{\perp})$ is the irreducible representation to which the charge-transfer transition moment (normal to the metal surface) belongs. For our case, since the molecule lies parallel to the metal surface, $\Gamma(\mu_{CT}^{\perp}) = A_2$. The lowest-lying allowed $\pi-\pi^*$ transition in CV is in the plane of the central C atom,[17] and therefore $\Gamma_K = E$. Thus, we expect that the most enhanced vibrational modes to be observed in SERS will be $A_2 \times E = e$ symmetry. Note that, in any case, totally symmetric a_1 modes are always enhanced due to *A*-term resonance contributions to the intensity, even if they are forbidden by the (*B*- or *C*-term) Herzberg−Teller-surface selection rules. This analysis shows that nontotally symmetric lines are most enhanced by proximity of CV to the metal surface, so much so that they come to dominate the spectrum. This is clear evidence of the importance of charge-transfer contributions to the SERS enhancements even in the single-molecule experiments.

Since the spectrum indicates strong Herzberg−Teller contributions to the intensity, it is important to determine if a CT resonance is energetically possible between the Ag surface and the adsorbed crystal violet molecule at the excitation wavelength. Electrochemical measurements can establish the approximate energies of highest occupied molecular orbital (HOMO) and lowest unoccupied molecular orbital (LUMO) levels of the molecule in solution from the reduction potentials of crystal violet cation for one-electron oxidation and reduction. These potentials have been determined in nonaqueous solvents where the electron-transfer reactions should be simple processes without chemical complications. For such a large molecule, the solvation energy differences between solvents should be small. For oxidation of CV^+, the half-wave potential was found to be +1.28 V versus Ag/AgCl reference in methylene chloride,[29] and for reduction it was found to be −0.59 V versus SCE in acetonitrile.[30] The two types of reference electrodes have almost the same reduction potential (+0.22 and +0.24 V, respectively). The potential of reduction corresponds energetically to the potential of maximum SERS intensity found in the study of Watanabe and Pettinger.[31] With the use of this data we obtain the energy level diagram shown in Figure 4.

The diagram shows that two simultaneous resonances are possible: a molecular resonance at around 2.0 eV (633 nm) and a CT (molecule-to-metal) resonance between the HOMO level

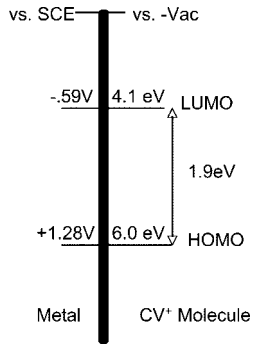

Figure 4. Energy level diagram showing levels in the CV^+ molecule vs the vacuum level and the corresponding levels in a metal electrode vs SCE reference. The relationship between the two energy scales is that the hydrogen reduction potential vs SCE is −0.24 V which corresponds to a Fermi level of −4.5 eV on an absolute scale.

and the potential-dependent Fermi level of the metal, at −0.59 eV (1.9 eV above the HOMO). The electrochemical HOMO−LUMO gap of 1.9 eV corresponds almost exactly to the origin of the lowest transition at 15 400 cm^{-1} in the experimental optical absorption spectra of CV^+.[32] We can also compare the energy levels from experiment with calculated values. The optimized DFT ground state with the CPCM water model shows two degenerate HOMO levels at −5.50 eV, and the TD-DFT calculations with the same model shows the first excited-state singlet transition of 2.47 eV with an oscillator strength of 0.81. Considering the approximations in excited-state calculations with density functionals which are optimized for ground-state calculations, these TD-DFT results are in good agreement with the electrochemically and optically determined energy levels of CV^+.

We have recently suggested a technique by which we can quantitatively estimate the magnitude of the contribution of charge transfer to the overall enhancement.[12,23] In the next section we apply this technique to CV to obtain a quantitative measure of this contribution.

IV. Degree of Charge Transfer in Crystal Violet SERS

We may define the degree of charge transfer for a particular normal mode (k) as

$$p_{CT}(k) = \frac{I^k(CT) - I^k(SPR)}{I^k(CT) + I^0(SPR)}$$

In this definition, I^k(CT) is the intensity of a spectral line in a region of the spectrum in which a charge-transfer resonance contributes to the SERS intensity. We also need two reference lines, measured in a region of the spectrum in which there are only contributions to the intensity from the SPR. I^0(SPR) is the intensity of a totally symmetric line, which is chosen as a reference. If the spectral line which is being examined (k) is totally symmetric, then I^k(SPR) = I^0(SPR). If it is not totally symmetric, then I^k(SPR) is the intensity of that line in the region where only the SPR contributes to the spectrum. Under normal circumstances, we expect this intensity to be small or zero, whereas we expect I^0(SPR) to be somewhat larger. In a recent work[33] we successfully applied the formula to several molecules, which were shown to have a substantial charge-transfer contribution to the SERS intensity. For CV we utilize the spectra obtained by Watanabe and Pettinger[31] in which SERS spectra were obtained electrochemically as a function of applied potential at 514.5 nm. In that work the potential dependence of many lines were examined, and plots of this dependence could

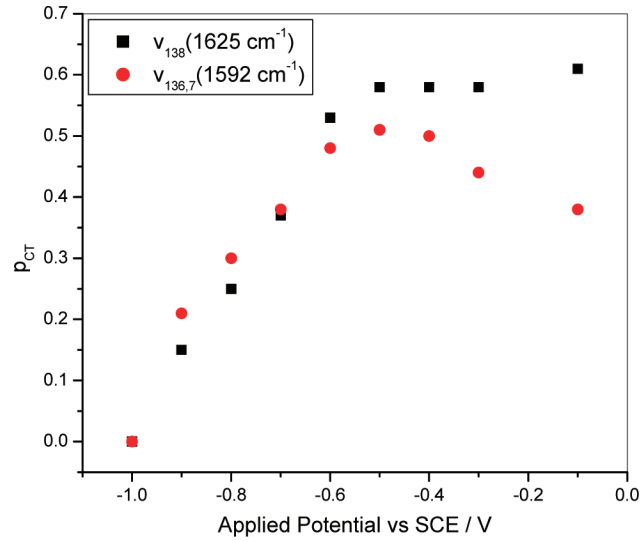

Figure 5. Degree of charge transfer in crystal violet as a function of applied potential.

be grouped into three types (see their Figure 3). The first two groups, labeled A and B, can be mostly assigned to e vibrations (see Table 1). (This A, B, and C, introduced by Watanabe and Pettinger, should not be confused with the A, B, and C terms of the Herzberg−Teller theory.) The B group exhibits a single peak at around −0.5 V, whereas the A group exhibits two apparent peaks, one at around −0.5 V, while as −0.1 V is approached, the intensity is increasing, presumably approaching a second peak at still more positive potential. The third pattern (C) is only reported for a single line at 1375 cm^{-1}, which corresponds to a benzene−N stretch of a_1 symmetry. The pattern for this line is flat between −0.1 and −0.6 V, and then drops off toward −1.0 V. This drop-off is most likely due to desorption of the molecule from the electrode surface or possible electroreduction in this potential range. The flat behavior is characteristic of a totally symmetric line[12] for which there is little contribution from the A term and no contribution from any totally symmetric transitions through intensity borrowing in the Herzberg−Teller B or C terms. We may therefore take this line as the totally symmetric reference line in the above equation. In order to account for the drop-off in intensity at more negative potentials, we will replace I^0(SPR) {normally a constant chosen at a potential at which there is no CT contribution} with its value as a function of potential, assuming there is no charge-transfer contribution to its value anywhere. For I^k(SPR) we take the intensity at −1.0 V.

In Figure 5 we plot the degree of charge transfer (p_{CT}) as a function of applied potential for a pair of lines {1625 cm^{-1} (ν_{138}) and 1592 cm^{-1} ($\nu_{136,137}$)}. Similar plots for all the other pairs reported by Watanabe and Pettinger[31] give nearly identical plots, and for space, we do not reproduce them here. As can be seen, starting at p_{CT} = 0 for −1.0 V, the degree of charge transfer increases rapidly until it reaches a maximum of around 0.5 at −0.5 V. After that it declines gradually for the line at 1592 cm^{-1}, but tends to increase for 1625 cm^{-1}, indicating the possibility of a second charge-transfer resonance beyond −0.1 V. It can be seen that these plots confirm that the contribution of charge transfer to the overall SERS enhancement is substantial, rising to more than 0.6 in one region of the potential curve. It is not clear exactly why there should be such a pronounced difference between the potential dependence of lines in the groups A and B. Presumably, as suggested by Watanabe and Pettinger, the difference arises from differing strengths of

Herzberg−Teller (vibronic) coupling between these two classes of vibrations, although this does not show up in the overall molecular symmetry when classified according to the D_3 point group. Note that Watanabe and Pettinger[31] identified the groups A and B as stemming from benzene-like vibrations of *a* and *b* symmetry, respectively. However, that assignment was based on the previous assignments of Angeloni et al.[20] Our revisions (see Table 1) do not support such a neat division, in that two of the *b* modes (8b and 16b) have been reclassified as *a* modes.

V. Conclusions

With the use of density functional calculations we have reassigned the spectrum of crystal violet. The resulting optimized structure is of point symmetry D_3 in agreement with the X-ray crystallographic results, and the calculated Raman spectrum provides an excellent match with the observed normal Raman spectrum. We are then able to present a reliable assignment of the symmetry and normal modes of the observed spectrum. In agreement with a previous Raman depolarization measurement, the assigned spectrum consists of a series of lines assigned to modes of either a_1 or *e* symmetry. The *e* modes are not split, either in the normal Raman spectrum or in SERS. Thus, the D_3 symmetry remains, even on the surface. We then show that the SERS spectra, both normal and single-molecule, are dominated by the nontotally symmetric *e* vibrations, which are selectively enhanced in accord with the Herzberg−Teller-surface selection rules. The mechanism involves intensity borrowing through vibronic coupling between a charge-transfer state and the lowest-lying $\pi \rightarrow \pi^*$ transition. We provide a quantitative measure of the degree of charge transfer by analyzing the potential dependence of SERS intensities and thereby show a considerable contribution of charge-transfer intensity to the overall SERS enhancement.

Acknowledgment. We acknowledge Irina Geiman for the recording of the FT-Raman and SERS spectra of crystal violet and Vasiliy Znenamenskiy for some DFT and TD-DFT calculations. We are also indebted to Dr. Marco Leona of the Metropolitan Museum of Art for invaluable assistance in this work. We are indebted to the National Institute of Justice (Department of Justice Award No. 2006-DN-BX-K034) and the City University Collaborative Incentive program (no. 80209). This work was also supported by the National Science Foundation under Cooperative Agreement No. RII-9353488, Grant Nos. CHE-0091362, CHE-0345987, and Grant No. ECS0217646 and by the City University of New York PSC−BHE Faculty Research Award Program. This research was also supported by a NASA sub-Grant from Radiation Monitoring Devices, Inc. and an NCSA Teragrid Grant CHE080072T for supercomputer facilities.

References and Notes

(1) Lombardi, J. R.; Birke, R. L.; Lu, T.; Xu, J. *J. Chem. Phys.* **1986**, *84*, 4174.
(2) Fleischmann, M.; Hendra, P. J.; McQuillan, A. J. *Chem. Phys. Lett.* **1974**, *26*, 163.
(3) McQuillan, A. J.; Hendra, P. J.; Fleischmann, M. *J. Electroanal. Chem.* **1975**, *65*, 933.
(4) Jeanmaire, D. L.; Van Duyne, R. P. *J. Electroanal. Chem.* **1977**, *84*, 1.
(5) Nie, S.; Emory, S. R. *Science* **1997**, *275*, 1102.
(6) Kneipp, K.; Wang, Y.; Kneipp, H.; Perelman, L.; Itzkan, I.; Dasari, R. R.; Feld, M. S. *Phys. Rev. Lett.* **1997**, *78*, 1667.
(7) Xu, H.; Bjerneld, E.; Käll, M.; Börjesson, L. *Phys. Rev. Lett.* **1999**, *83*, 4357.
(8) LeRu, E. C.; Blackie, E.; Meyer, M.; Etchegoin, P. G. *J. Phys. Chem. C* **2007**, *111*, 13794–13803.
(9) Michaels, A. M.; Jiang, J.; Brus, L. E. *J. Phys. Chem. B* **2000**, *104*, 11965.
(10) Bosnick, K. A.; Jiang, J.; Brus, L. E. *J. Phys. Chem. B* **2002**, *106*, 8096.
(11) Kneipp, K.; Kneipp, H.; Kartha, V. B.; Manoharan, R.; Deinum, G.; Itzkan, I.; Dasari, R. R.; Feld, M. S. *Phys. Rev. E* **1998**, *57*, R6281.
(12) Lombardi, J. R.; Birke, R. L. *J. Phys. Chem. C* **2008**, *112*, 5605–5617.
(13) Arenas, J. F.; Wooley, M. S.; Otero, J. C.; Marcos, J. I. *J. Phys. Chem.* **1996**, *100*, 3199.
(14) Albrecht, A. C. *J. Chem. Phys.* **1960**, *34*, 1476.
(15) Hildebrandt, P.; Stockburger, M. *J. Phys. Chem.* **1984**, *24*, 5935.
(16) Gomes de Mesquita, A. H.; MacGillavry, C. H.; Eriks, K. *Acta Crystallogr.* **1965**, *18*, 437.
(17) Dekkers, H. P. J. M.; Kielman-Van Luyt, E. C. M. *Mol. Phys.* **1976**, *31*, 1001.
(18) Liang, E. J.; Ye, X. L.; Kiefer, W. *J. Phys. Chem. A* **1997**, *101*, 7330.
(19) Lovell, S.; Marquandt, B. J.; Kahr, B. *J. Chem. Soc., Perkin Trans. 2* **1999**, 2241.
(20) Angeloni, L.; Smulevich, G.; Marzocchi, M. P. *J. Raman Spectrosc.* **1979**, *8*, 305.
(21) Sunder, S.; Bernstein, H. J. *Can. J. Chem.* **1981**, *59*, 964.
(22) Lueck, H. B.; McHale, J. L.; Edwards, W. D. *J. Am. Chem. Soc.* **1992**, *114*, 2342.
(23) Wang, M.; Teslova, T.; Xu, F.; Lombardi, J. R.; Birke, R. L.; Leona, M. *J. Phys. Chem. C* **2007**, *111*, 3044.
(24) Teslova, T.; Corredor, C.; Livingstone, R.; Spataru, T.; Birke, R. L.; Lombardi, J. R.; Canamares, M. V.; Leona, M. *J. Raman Spectrosc.* **2007**, *38*, 802.
(25) Wang, M.; Spataru, T.; Lombardi, J. R.; Birke, R. L. *J. Phys. Chem. C* **2007**, *111*, 3038.
(26) Leona, M.; Lombardi, J. R. *J. Raman Spectrosc.* **2007**, *38*, 853.
(27) Lee, P. C.; Meisel, D. *J. Phys. Chem.* **1982**, *86*, 3391.
(28) Frisch, M. J.; Trucks, G. W.; Schlegel, H. B.; Scuseria, G. E.; Robb, M. A.; Cheeseman, J. R.; Montgomery, J. A., Jr.; Vreven, T.; Kudin, K. N.; Burant, J. C.; Millam, J. M.; Iyengar, S. S.; Tomasi, J. J.; Barone, V.; Mennucci, B.; Cossi, M.; Scalmani, G.; Rega, N.; Petersson, G. A.; Nakatsuji, H.; Hada, M.; Ehara, M.; Toyota, K.; Fukuda, R.; Hasegawa, J.; Ishida, M.; Nakajima, T.; Honda, Y.; Kitao, O.; Nakai, H.; Klene, M.; Li, X.; Knox, J. E.; Hratchian, H. P.; Cross, J. B.; Adamo, C.; Jaramillo, J.; Gomperts, R.; Stratmann, R. E.; Yazyev, O.; Austin, A. J.; Cammi, R.; Pomelli, C.; Ochterski, J. W.; Ayala, P. Y.; Morokuma, K.; Voth, A.; Salvador, P.; Dannenberg, J. J.; Zakrzewski, V. G.; Dapprich, S.; Daniels, A. D.; Strain, M. C.; Farkas, O.; Malick, D. K.; Rabuck, A. D.; Raghavachari, K.; Foresman, J. B.; Ortiz, J. V.; Cui, Q.; Baboul, A. G.; Clifford, S.; Cioslowski, J.; Stefanov, B. B.; Liu, G.; Liashenko, A.; Piskorz, P.; Komaromi, I.; Martin, R. L.; Fox, D. J.; Keith, T.; Al-Laham, M. A.; Peng, C. Y.; Nanayakkara, A.; Challacombe, M.; Gill, P. M. W.; Johnson, B.; Chen, W.; Wong, M. W.; Gonzalez, C.; Pople, J. A. Gaussian 03, revision C.02; Gaussian, Inc.: Wallingford, CT, 2004.
(29) Kobotaeva, N. S.; Sirotkina, E. E.; Mikubaeva, E. V. *Russ. J. Electrochem.* **2006**, *42*, 268.
(30) Compton, R. G.; Wellington, R. G. *J. Phys. Chem. C* **1994**, *98*, 270.
(31) Watanabe, T.; Pettinger, B. *Chem. Phys. Lett.* **1982**, *89*, 501.
(32) Beck, M. E. *Int. J. Quantum Chem.* **2005**, *101*, 683.
(33) Chenal, C.; Birke, R. L.; Lombardi, J. R. *ChemPhysChem* **2008**, *9*, 1617.

JP807807J